Prell, W.L., Wang, P., Blum, P., Rea, D.K., and Clemens, S.C. (Eds.)
Proceedings of the Ocean Drilling Program, Scientific Results Volume 184

11. ABUNDANCE VARIATIONS OF PLANKTONIC FORAMINIFERS DURING THE MID-PLEISTOCENE CLIMATE TRANSITION AT ODP SITE 1144, NORTHERN SOUTH CHINA SEA[1]

Fan Zheng,[2] Qianyu Li,[3,4] Xia Tu,[2] Muhong Chen,[2] Baohua Li,[5] and Zhimin Jian[3]

ABSTRACT

The abundances of planktonic foraminifers are documented in samples from the interval between 300 and 518 meters composite depth at Site 1144, northern South China Sea. With resolution of ~500–1000 yr, this work represents the first high-resolution study of the climate changes between 0.5 and 1.0 Ma recorded in planktonic foraminifers from the western Pacific. Faunal responses at this site to orbital forcing of climate variations during the mid-Pleistocene transition are found to have been mainly gradual and progressive, accompanied by swift shifts in the abundances of some individual species. Warm-water species represented by *Globigerinoides* spp. decrease from an average of 60% in marine isotope Stage (MIS) 29 and older intervals to <40% at MIS 22, followed by a steady increase in cool-water species toward younger intervals. Cool-water species including *Neogloboquadrina pachyderma* and *Globorotalia inflata* increased from <20% prior to MIS 23 to >35% in MIS 15 and 14. The deep-dwelling warm-water species *Sphaeroidinella dehiscens* decreased to a minimum during MIS 22 and remained extremely rare, 0%–4%, throughout the upper part of the section. This contrast is also reflected in the estimated sea-surface temperature, which shows a maximum winter temperature difference of 11°C (17°–28°C) during MIS 22. Since then, a stronger association started to de-

---

[1] Zheng, F., Li, Q., Tu, X., Chen, M., Li, B., and Jian, Z., 2006. Abundance variations of planktonic foraminifers during the mid-Pleistocene climate transition at ODP Site 1144, northern South China Sea. *In* Prell, W.L., Wang, P., Blum, P., Rea, D.K., and Clemens, S.C. (Eds.), *Proc. ODP, Sci. Results,* 184, 1–21 [Online]. Available from World Wide Web: <http://www-odp.tamu.edu/publications/184_SR/VOLUME/CHAPTERS/222.PDF>. [Cited YYYY-MM-DD]

[2] South China Sea Institute of Oceanology, Chinese Academy of Sciences, Guangzhou 510301, People's Republic of China.
[3] Key Laboratory of Marine Geology DoE, Tongji University, Shanghai, 200092, People's Republic of China.
[4] School of Earth and Environmental Sciences, The University of Adelaide, Adelaide SA 5005, Australia.
qianyu.li@adelaide.edu.au
[5] Nanjing Institute of Geology and Paleontology, Chinese Academy of Sciences, Nanjing 210008, People's Republic of China.

Initial receipt: 18 December 2002
Acceptance: 10 August 2005
Web publication: 22 February 2006
Ms 184SR-222

velop between species abundance fluctuations and glacial–interglacial cycles. These planktonic foraminifer changes during MIS 22 mark the mid-Pleistocene revolution (MPR) at 0.9 Ma. The MPR event also led to a well-stratified upper water column and a more constrained thermocline, as indicated by abundance changes of deep-dwelling species. The major cooling at MIS 16 almost completely eliminated such deep-dwelling warm-water species as *Globorotalia tumida*. The planktonic foraminifer results from Site 1144 sample orbital forcing climate changes from 41 to 100 k.y. cyclicities during the mid-Pleistocene climate transition.

INTRODUCTION

Site 1144 is located at 20°3.18′ N, 117°25.14′ E, at a water depth of ~2037 m, which is above the sill depth of the Bashi Strait (2600 m) (Fig. F1). Modern sea-surface temperature (SST) in the area is 28.8°C in summer and ~23.5°C in winter, and the depth of thermocline is at ~120 m (Pflaumann and Jian, 1999). Three holes were drilled to 519.19 meters composite depth (mcd), and the oldest sediment recovered is of early Pleistocene age. Sedimentation rates at this site are extremely high because of its vicinity to the Pear River mouth in the northern South China Sea (Wang, Prell, Blum, et al., 2000): 930 m/m.y. for the last 0.3 m.y. and ~390 m/m.y. between 0.3 and 1.0 Ma. With excellent 100% core recovery, this thick sediment succession is ideal for high-resolution studies of fine-scale paleoclimatic and paleoceanographic changes in the region.

F1. Site locations, p. 13.

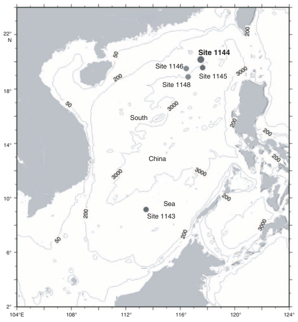

The hemipelagic sediments are characterized by fine-grained clay-sized terrigenous material, quartz silt, calcareous nannofossils, and foraminifers with frequent black iron sulfide mottling and pyrite. A microtectite layer found at 386 mcd records a large-scale meteorite impact in the region at ~0.78 Ma (Glass, 1967; Zhao et al., 1999).

We conducted a postcruise study on planktonic foraminifers from cores below 300 mcd at Site 1144, aiming to quantify the abundance variations of planktonic foraminifer species and to provide evidence of high-resolution faunal responses to the mid-Pleistocene climate transition in the northern South China Sea.

MATERIAL AND METHODS

A total of 475 samples from 300.82 to 518.11 mcd at Site 1144 were used in this study. Sampling spacing varies from 30 cm between 300.82 and 415.58 mcd to 50–70 cm between 415.58 and 518.11 mcd. Three intervals lack samples because of either incomplete core recovery or contamination: 352–357 mcd, 365–370 mcd, and 387–391 mcd. On the basis of isotopic stratigraphy, the time resolution of these samples varies from 500–1000 yr.

Samples were processed with standard techniques. Residue >63 µm was collected and separated into two fractions using a 150-µm sieve. More than 300 planktonic foraminifers from a portion of the >150-µm fraction were picked and identified, and the percentage abundances of various species were calculated and charted. We followed the species taxonomy of Kennett and Srinivasan (1983), Bolli and Saunders (1985), and Hemleben et al. (1989). Species preferences to climate belts or faunal provinces, as summarized by Bé (1977), were used for grouping species.

Test fragments were also counted. Fragmentation results based on eight fragments equaling one complete test were used to infer carbonate dissolution in the bottom water (Le and Shackleton, 1992). Coarse fraction data show higher percentages in glacial intervals than in interglacial intervals, indicating stronger offshore transport at sea level lowstands (Fig. **F2**).

SST was estimated using paleoecology transfer function FP-12E of Thompson (1981) on planktonic foraminifer census data (see the **"Appendix"**). The method developed by Pflaumann and Jian (1999) was not employed because it often underestimates the winter SST because of few modern analogs from high latitudes. Figures **F2, F3, F4, F5,** and **F6** illustrate the isotopic and coarse fraction results as well as the abundance profiles of common species documented in this study.

RESULTS

General Characteristics of the Planktonic Foraminifer Assemblage

At least 5%–10% of planktonic foraminifer tests are seriously affected by dissolution and became fragmented. More fragments are found in interglacial intervals (maximum = 60%–80%) than in glacial intervals (mostly 10%–15%). There are exceptions, however, with up to 30%–40% fragmented tests from some glacial intervals (Fig. **F2**).

Except where dissolution prevails, planktonic foraminifers are abundant and well preserved in most samples studied. The absolute abundance varies from <30 to >400 specimens/g of dried sample. (Fig. **F2**). More species and specimens are recorded in interglacial intervals than in glacial intervals, but the absolute abundance may increase to 300–500 specimens/g at some levels of glacial marine isotope Stages (MIS) 16 and 22, signaling sudden blooms of certain cool-water forms.

Representing the subtropical province (Bé, 1977), the planktonic foraminifer assemblage is dominated by *Globigerinoides* (*Globigerinoides ruber* and *Globigerinoides sacculifer*) and *Globorotalia* (warm-water *Globorotalia menardii* and cool-water *Globorotalia inflata*) and *Neogloboquadrina* (mainly *Neogloboquadrina dutertrei*). There is a major shift in the abundance of warm and cool groupings at ~420 mcd, with warm species averaging >50% below this level and cool-water individuals increasing their average abundance to 35% or more above this level. Fluctuations are evident in all groupings, and they are mainly related to the alternation of glacial–interglacial cycles (Figs. **F3, F4, F5**).

Geochronologic Framework and Useful Species Datum Levels

The shipboard geochronologic framework for Site 1144 was mainly based on nannofossil and planktonic foraminifer biostratigraphy and geomagnetostratigraphy (Wang, Prell, Blum, et al., 2000). The age model has since been refined by postcruise isotopic studies (**Bühring et al.,** this volume). The isotopic results indicate that the interval between 300 and 500 mcd fall in MIS 14–29, representing sedimentation in the past 0.5–1.0 m.y. (Table **T1**).

F2. Foraminifer abundance, 300–518 mcd, p. 14.

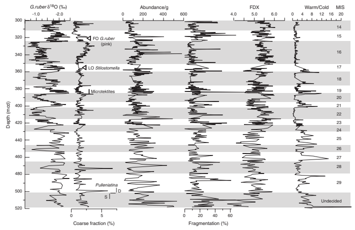

F3. Warm-water foraminifer abundance profiles, p. 15.

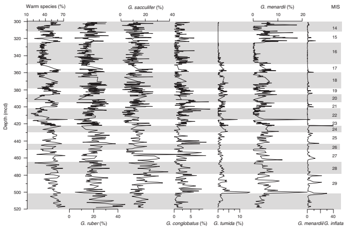

F4. Cool- to cold-water foraminifer abundance profiles, p. 16.

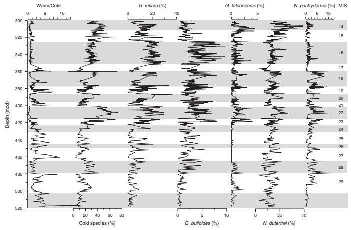

F5. Deep-dwelling foraminifer abundance profiles, p. 17.

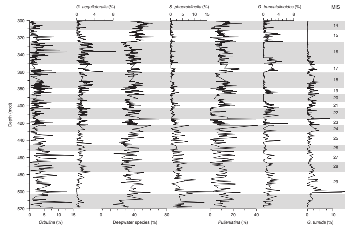

F6. Time plots, p. 18.

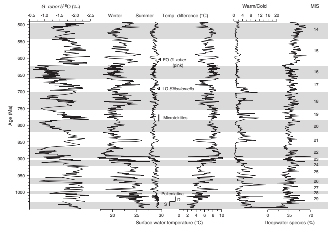

T1. MIS positioning, p. 20.

Several biostratigraphically useful foraminifer events were also observed (Table **T1**). In descending order, they are as follows:

1. The first occurrence (FO) of pink *G. ruber* at 313 mcd is in the lower part of MIS 14. This datum bears an age of ~0.55 Ma, about 0.13 m.y. older than its consistent occurrence level dated previously at 0.42 Ma (Li, 1997; Wang, Prell, Blum, et al., 2000).
2. The last occurrence (LO) of *Stilostomella* at ~356 mcd is in the lower part of MIS 17 with an age of ~0.69 Ma, or ~0.07 m.y. older than the record of 0.62 Ma from other tropical Indo-Pacific regions (Schönfeld, 1996) but ~0.06 m.y. younger than the 0.75 Ma dated at Site 1143 in the southern South China Sea (Wang, Prell, Blum, et al., 2001).
3. At 500.50 mcd, the coiling direction in *Pulleniatina obliquiloculata* changed from sinistral to dextral. This probably marks the last such coiling change in this taxon and occurred ~1.6 m.y. ago (Kennett and Srinivasan, 1983; G.X. Qin, 2002, pers. comm.). This finding may have two implications: (1) the bottom part of the core at Site 1144 (519 mcd) could have an age of ~1.7 Ma or older (rather than 0.9 Ma as suggested in the Leg 184 *Initial Reports* volume) and (2) a hiatus lasting up to 0.6 m.y. (between 1.0 and 1.6 Ma) could have occurred near the 500-mcd level. Immediately above this level, at 499.19 mcd, the LO of the small *Gephyrocapsa* acme has been dated as representing 1.01 Ma (Wang, Prell, Blum, et al., 2000). An age >1.0 Ma for the bottom part of Site 1144 is also supported by *Neogloboquadrina humerosa*, a late Miocene to early Pleistocene species (8.5–1.3 Ma) found mainly in intervals below 479.86 mcd. In the following, however, we refer to the intervals below 500 mcd as "intervals older than MIS 29" pending further studies of its exact age.

The isotope results by **Bühring et al.** (this volume) indicate that the mid-Pleistocene revolution (MPR) (0.9 Ma) lies at ~418 mcd, close to the MIS 22/23 boundary (Fig. **F2**). Moreover, the Brunhes/Matuyama boundary, which was not well defined in the Leg 184 *Initial Reports* volume, should be tuned to 386 mcd to coincide with the early part of MIS 19. Abundant microtectites were also observed at a similar level (~386 mcd), representing the meteorite impact event widely recorded in the Indo-Pacific region (Glass, 1967; Zhao et al., 1999). These two events appear to have concurred at ~0.78 Ma (Fig. **F2**).

Abundance of Planktonic Foraminifer Species

Globigerina bulloides d'Orbigny

Remarks: *Globigerina bulloides* is extremely rare (0%–3%) in the bottom 40 and top 20 m of the studied section. Its abundance increases to 5% or more in glacial cycles, especially MIS 16, 18, 20, and 22, between 320 and 420 mcd. Interestingly, a similar percentage is also recorded from the upper part of MIS 19 and 17, where other cool-water forms such as *Globorotalia inflata* and *Neogloboquadrina pachyderma* also register relatively high abundances (Fig. **F4**).

Globigerina falconensis Blow

Remarks: Similarly rare as *G. bulloides*, *G. falconensis* appears to be less influenced by glacial–interglacial alternations. After MIS 19, however, its abundance maxima (2.5%–4%) always occurs during interglacials (Fig. **F4**).

Globigerinella aequilateralis (Brady)

Remarks: Rare throughout the section, *G. aequilateralis* constitutes only 2% or less in the lower part of the section, increasing to 3% or more after MIS 19, and peaking at two levels within MIS 18 and 16 with over 4% abundance. It decreases again upsection in MIS 15 and 14 (Fig. **F5**).

Globigerinoides ruber (d'Orbigny)

Remarks: As a typical subtropical species, *G. ruber* is frequent to abundant, averaging 18%–20%. A maximum abundance of >40% is found at 510 mcd. Generally, its abundance curve shows a parallel trend with isotopic fluctuations, although details vary and the trend may reverse to high *G. ruber* abundance in some parts of glacial intervals, such as in upper MIS 26 and lower MIS 20 (Fig. **F3**).

Globigerinoides sacculifer (Brady)

Remarks: This tropical–subtropical species is more frequent between 455 and 490 mcd (average = 20%) than in other intervals (average = 15%). A maximum abundance of ~50% occurs at 457 mcd. Low *G. sacculifer* abundance associated with glacial intervals, however, is evident only after MIS 23 (above 420 mcd), and its abundance increased in the upper parts of MIS 18, 16, and 14 (Fig. **F3**).

Globigerinoides conglobatus (Brady)

Remarks: Unlike *G. ruber* and *G. sacculifer, G. conglobatus* is rare, often <5%. Its abundance increases to >7% only in MIS 21 and older interglacial stages (Fig. **F3**).

Globorotalia menardii Parker, Jones, and Brady

Remarks: This tropical–subtropical species shows distinct correlation with interglacial cycles above 420 mcd, but such a positive correlation is vague from below this level, although several abundance peaks all fall within interglacial intervals. It is extremely rare or even absent from upper MIS 22, mid-20, upper 18, upper 17, 16, and lower 14 (Fig. **F3**).

Globorotalia truncatulinoides (d'Orbigny)

Remarks: This deepwater thermocline dweller is rare, 4% or less, in most samples. Its abundance may increase to 4% or more in interglacial stages but decreases even to zero in interglacial intervals. A close association with glacial–interglacial fluctuations is more eminent after MIS 22 (above 410 mcd) (Fig. **F5**).

Globorotalia inflata d'Orbigny

Remarks: Rare to frequent *G. inflata*, mainly 10% or less, occurs below 420 mcd and in interglacial to glacial transitions above this level. Its overall abundance increases significantly above this level, reaching 25%-30% at upper MIS 22, upper 20, upper 19, upper 17, lower 16, upper 16, and lower 15 (Fig. **F4**).

Other *Globorotalia*

Remarks: These include *Globorotalia tumida* (Brady) and *Globorotalia hirsuta* (d'Orbigny). They are rare, each rarely exceeding 3%, and occur mainly in interglacial intervals (Fig. **F5**). Comparatively, *G. hirsuta* has a more discontinuous range.

Neogloboquadrina dutertrei (d'Orbigny)

Remarks: This species shows a steady increase upsection in its average abundance, from ~15% below 420 mcd to 20%–25% between 420 and 320 mcd, to >30% between 320 and 300 mcd. Its low abundance often occurs at glacial–interglacial or interglacial–glacial transitions, while its abundance maxima are mainly confined to glacial cycles, especially MIS 14, 16, 20, 22, and 26 (Fig. **F4**).

Neogloboquadrina humerosa (Takayanagi and Saito)

Remarks: Rare typical *N. humerosa* mainly occurs below 440 mcd, becoming more frequent below 500 mcd.

Neogloboquadrina pachyderma (Ehrenberg)

Remarks: This cold-water species is rare, often <5%, except in lower MIS 29, upper 22, upper 19, and upper 18, where its abundance may reach 10% or more (Fig. F4).

Orbulina universa d'Orbigny

Remarks: Except at several interglacial levels where its abundance exceeds 10%, *O. universa* attains only 2%–5% of the total planktonic foraminifer assemblage in most samples. Above 420 mcd, it remains frequent in MIS 21, 19, upper 18, 16, and lower 15 (Fig. F5).

Pulleniatina obliquiloculata (Parker and Jones)

Remarks: The abundance of this subtropical species varies from <5% to >15%, with two abundance pulses of ~40% at 415 and 422 mcd. Its abundance fluctuations are often associated with glacial–interglacial cycles, but this coherence is less obvious from below 420 mcd, prior to MIS 20 (Fig. F5).

Sphaeroidinella dehiscens (Parker and Jones)

Remarks: This tropical–subtropical dissolution-resistant species is rare (0%–3%) above 420 mcd, increasing occasionally to 5% or more downhole. Its abundance peaks occur in both glacials (upper MIS 24 and upper 26) and interglacials (mid-MIS 25, mid-27, and mid-29) (Fig. F5).

DISCUSSION

Glacial–Interglacial Faunal Contrasts during the Mid-Pleistocene Transition

A good correlation exists between planktonic foraminifer changes and the oxygen isotopic record (Figs. F2, F3, F4, F5). If the isotope record indeed chiefly reflects the waning and waxing of polar ice, the planktonic foraminifer results reported here must have resulted from global ice volume changes through glacial–interglacial cycles. Prior to 0.9 Ma (below 420 mcd), however, this relationship was vague for many individual species. Abundant warm-water species occur below 420 mcd, indicating a much warmer climate regime before the MPR. This warm climate regime caused relatively smaller glacial–interglacial contrasts and smaller summer–winter SST differences than after 0.9 Ma. The estimated SST using transfer function FP-12E shows an average difference of 7.5°C between summer and winter SST (28.5°–21.0°C) for the 300- to 420-mcd interval. The strongest winter SST differences occurred between 410 and 422 mcd, in MIS 23 to lower 22, bracketing the MPR event (Fig. F6). The pre-MPR warm climate regime changed gradually, however, as indicated by increases upsection of cool-water species including *G. bulloides* and *G. inflata*.

In spite of being relatively warm before the MPR, glacial–interglacial transitions appear to have been rapid. The total warm- to cold-water species ratio and *G. menardii* to *G. inflata* ratio both show sudden jumps, indicating rapid transitions across glacial/interglacial boundaries (Fig. F4). These rapid changes from one climate stage to another continued into younger periods, although the overall climate has shifted to one dominated by much cooler conditions with more abundant cool-water species after the MPR.

The SST differences enlarged after the MPR, accompanied by stronger glacial–interglacial contrasts in planktonic foraminifer abundances. This shift appears to be mainly influenced after the MPR by much cooler winters driven by stronger glaciations. The cooler climate regime started affecting planktonic foraminifers immediately after the MPR, and climate deteriorations, began early even in the later part of interglacials and continued across interglacial/glacial boundaries. For instance, abundance of cool- to cold-water species such as *G. bulloides, G. pachyderma,* and *G. inflata* increased in the later part of MIS 21, 19, and 17, although the increases were not always simultaneous or at a similar amplitude (Fig. F4). These progressive changes in planktonic foraminifer response to interglacial–glacial transitions mimic the pattern of changes from MIS 5–2 (Wang and Wang, 1990; Wang, 1999; Wang et al., 1999; Jian et al., 2000b), indicating that such typical late Pleistocene interglacial–glacial transitions first began ~0.9 m.y. ago, immediately after the MPR. In contrast, faunal changes from glacial–interglacial cycles were rapid after the MPR, especially between MIS 22 and 17, as indicated by the warm- to cool-species ratio (Fig. F4).

As recorded elsewhere, the first strongest glaciation in the last 1 m.y. occurred at MIS 16, which dwarfed all tropical–subtropical species while encouraging an exceptionally high production of cool-water species at Site 1144 (Fig. F4). The impact of this glaciation continued into the subsequent interglacial MIS 15 and glacial MIS 14 with minimal recovery of warm-water species.

Upper Water Stratification and Thermocline

Several planktonic foraminifer species are good indicators of upper water stratification because they are found living mainly in certain layers of the world ocean. *G. ruber* is a typical surface water species living in the upper 50 m of the water column, whereas globorotaliid forms are more frequent in deeper waters with relative heavy $\delta^{18}O$ (Fairbanks et al., 1982; Helemben et al., 1989). Surface-water species increased in abundance when the thermocline deepened, and vice versa for those deepwater dwellers including *Globorotalia, Pulleniatina,* and *Sphaeroidinella* (Anderson and Ravelo, 1997; Jian et al., 2000a, 200b).

Figure F5 shows abundance variations of the deep-dwelling group and its major constituents, apart from *G. aequilateralis* and *Orbulina* spp., which are ubiquitous in the tropics and subtropics. The total abundances of the deep-dwelling group fluctuate mainly between 30% and 50% throughout the studied interval, indicating that the overall upper water structure in the northern South China Sea has been stable during the early and mid-Pleistocene. The abundance variations of these deep dwellers, however, did not responded well to glacial–interglacial cycles until MIS 21, immediately before the MPR. Only after MIS 21 did all deep dwellers exhibit a close relationship with isotopic fluctuations. The increase in *P. obliquiloculata* and *G. menardii* groups during interglacials at and after MIS 21 likely indicate the development of a well-constrained thermocline that shoaled during interglacials and deepened during glacials. In contrast, *S. dehiscens* decreased substantially after MIS 23, and since then its abundance has remained extremely low. The reductions of *S. dehiscens* after MIS 23 and *G. tumida* after MIS 17 were probably due to a cooler climate regime and weaker warm currents, as indicated also by the decrease in many shallow-dwelling warm-water species close to the MPR (Fig. F3).

Therefore, planktonic foraminifer response to the mid-Pleistocene transition was gradual and progressive, with species abundance changes occurring before, at, and after the MPR. It is not clear, however, whether and how much these faunal variations were influenced by the dynamics of Asian monsoons and/or of the Western Pacific Warm Pool during the mid-Pleistocene climate transition.

Astronomically Forcing Faunal Responses to Climate Change

The MPR marks the transition from 41- to 100-k.y. cyclicities, shaping the general pattern of the two-moded Quaternary climate as recorded in deep-sea oxygen isotopes (Prell, 1982; Berger et al., 1993; Raymo et al., 1997; Schmieder et al., 2000; Wang et al., 2001). The orbital forcing is also reflected in individual planktonic foraminifers. Figure **F7** shows the results of spectrum analysis on four of the most common species using the method described by Schulz and Stattegger (1997). A prominent eccentricity band represented by 80- to 100-k.y. cycles occurs in all four species, most pronouncedly in *G. ruber.* The obliquity (39–41 k.y.) and precession (19–23 k.y.) cycles and many shorter cycles are also strong, indicating orbital and local climatic forcings including tropical monsoons. For instance, the missing 41-k.y. cycle in *G. sacculifer* may have been caused by the disturbance of monsoons. Although the MPR is not obvious in Figure **F7** because the studied interval is too short to be separated into two sections (before and after 0.9 Ma) for spectrum analysis, these results still demonstrate that (1) faunal responses to orbital forcing climatic changes are different in both frequencies and amplitude, and (2) local factors represented by shorter cycles could have also played an important role.

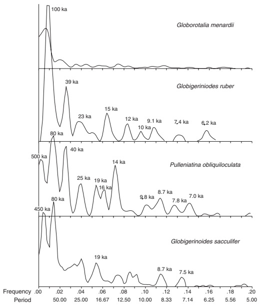

F7. Planktonic species spectrum analysis, p. 19.

Comparison between Northern and Southern South China Sea Records

Jian et al. (2000b) reported foraminifer responses to the mid-Pleistocene climate transition in Core 17957 (10°53.9′ N, 115°18.3′ E; water depth = 2195 m), in the southern South China Sea. Similar to the results presented above, planktonic foraminifers from Core 17957 show immediate changes in water temperature and thermocline depth at 0.9 Ma, but the benthic foraminifers did not change much until the Brunhes/Matuyama reversal. In the same core, radiolarian abundances also changed close to the MPR, characterized by a decrease in tropical species (Wang and Albermann, 2002). These authors attribute the changes in plankton to a southward shift of the North Equatorial Current likely induced by variations in the northern trade wind system during the MPR, about 0.9 m.y. ago.

At Site 1143 (9°21.72′ N, 113°17.11′ E; water depth = 2772 m), planktonic foraminifer changes were also in path with a progressive mid-Pleistocene climatic transition (MPT). The most striking feature, however, is that the abundance of *P. obliquiloculata* became reversed from high in interglacials before the MPR to high in glacials after the MPR (Xu et al., 2005). As *P. obliquiloculata* prefers high salinity, its high abundance in glacials after the MPR could have been because of high salinity in the southern South China Sea when sea level was as much as 120 m lower than today’s, the basin was semienclosed, and evaporation was high. This phenomenon, however, does not exist in the northern South China Sea, including Site 1144, probably because a consistent influence of the west Pacific water through the Bashi Strait (–2600 m) and more frequent winter monsoons during glacial and interglacial periods.

SUMMARY

For the first time in the western Pacific, planktonic foraminifer responses to the MPT at an average resolution of 500–1000 yr were studied in 475 samples taken from the 300- to 518-mcd interval of Site 1144, northern South China Sea. The studied interval covers MIS 14–29, with an undecided age for the bottom part of the section below 500 mcd. Abundant warm-water species typified by *Globigerinoides* occur in the lower part of the section, with 60% average abundance from MIS 29 and older intervals. Their abundances decrease to <40% during MIS 22 and younger glacial periods. In contrast, cool- and cold-water species including *G. bulloides, N. pachyderma,* and *G. inflata* increase from <20% prior to MIS 23 to >35% in MIS 15 and 14. The deep-dwelling warm-water species *S. dehiscens* decreased to minimum during MIS 22 and remained extremely rare (0%–4%) throughout the upper part of the section. These planktonic foraminifer changes across the MIS 22/23 boundary mark the mid-Pleistocene revolution at 0.9 Ma.

Paleo-SST estimated using transfer function FP-12E shows smaller changes in summer and winter temperatures and their difference before the MPR. The average SST was 29°C for summer and 23.6°C for winter before the MPR but changed to 28.5°C and 21°C, respectively, after the MPR. A maximum winter temperature difference of 11°C (17°–28°C) was recorded during MIS 22.

As indicated by deep-dwelling species, the MPR event also led to a well-stratified upper water column and a more constrained thermocline that fluctuated neatly with glacial–interglacial cycles after 0.9 Ma. Beginning from the MPR, a stronger association started to develop between fluctuations of species abundances and glacial–interglacial cycles. The great cooling at MIS 16 almost completely eliminated several deep-dwelling warm-water species including *G. tumida*. Most planktonic foraminifer species exhibit abundance changes closely coherent with climate transition from 41- to 100-k.y. cyclicities, as well as with fluctuations of glacial–interglacial cycles. Although marked by a profound shift in some individual species across the MPR, the overall planktonic foraminifer responses to orbital forcing climate changes during the mid-Pleistocene transition were gradual and progressive.

ACKNOWLEDGMENTS

This research used samples and/or data provided by the Ocean Drilling Program (ODP). ODP is sponsored by the U.S. National Science Foundation (NSF) and participating countries under management of Joint Oceanographic Institutions (JOI), Inc. Funding for this research was provided by grants from the National Natural Science Foundation of China, Chinese Academy of Sciences, and Australian Research Council. The manuscript was reviewed by two anonymous reviewers.

REFERENCES

Anderson, D.J., and Ravelo, A.C., 1997. Tropical Pacific Ocean thermocline depth reconstructions for the Last Glacial Maximum. *Paleoceanography,* 12:395–413.

Bé, A.W.H., 1977. An ecological, zoogeographic and taxonomic review of Recent planktonic foraminifera. *In* Ramsey, A.T.S. (Ed.), *Oceanic Micropaleontol.,* 19:150–192.

Berger, W.H., Bickert, T., Jansen, E., Wefer, G., and Yasuda, M., 1993. The central mystery of the Quaternary ice age. *Oceanus,* 36:53–56.

Bolli, H.M., and Saunders, J.B., 1985. Oligocene to Holocene low latitude planktic foraminifera. *In* Bolli, H.M., Saunders, J.B., and Perch-Nielsen, K. (Eds.), *Plankton Stratigraphy:* Cambridge (Cambridge Univ. Press), 155–262.

Fairbanks, R.G., Sverdlove, M., Free, R., Wiebe, P.H., and Bé, A.W.H., 1982. Vertical distribution and isotopic fractionation of living planktonic foraminifera from the Panama Basin. *Nature (London, U. K.),* 298:841–844.

Glass, B., 1967. Microtektites in deep-sea sediments. *Nature (London, U. K.),* 214:373–374.

Hemleben, C., Spindler, M., and Anderson, O.R., 1989. *Modern Planktonic Foraminifera:* Berlin (Springer-Verlag).

Jian, Z., Li, B., Huang, B., and Wang, J., 2000a. *Globorotalia trucatulinoides* as indicator of upper-ocean thermal structure during the Quaternary: evidence from the South China Sea and Okinawa Trough. *Palaeogeogr., Palaeoclimatol., Palaeoecol.,* 162:287–298.

Jian, Z., Wang, P., Chen, M., Li, B., Zhao, Q., Bühring, C., Laj, C., Lin, H., Pflaumann, U., Bian, Y., Wang, R., and Cheng, X., 2000b. Foraminiferal responses to major Pleistocene paleoceanographic changes in the southern South China Sea. *Paleoceanography,* 15:229–243.

Kennett, J.P., and Srinivasan, M.S., 1983. *Neogene Planktonic Foraminifera: A Phylogenetic Atlas:* Stroudsburg, PA (Hutchinson Ross).

Le, J., and Shackleton, N.J., 1992. Carbonate dissolution fluctuations in the western equatorial Pacific during the late Quaternary. *Paleoceanography,* 7(1):21–42.

Li, B., 1997. Paleoceanography of the Nansha area, southern South China Sea since the last 700,000 years [Ph.D. dissert.]. Nanjing Inst. Geol. Paleontol., Academic Sinica, Nanjing, China. (in Chinese, with English abstract)

Pflaumann, U., and Jian, Z., 1999. Modern distribution patterns of planktonic foraminifera in the South China Sea and western Pacific: a new transfer technique to estimate regional sea-surface temperatures. *Mar. Geol.,* 156:41–83.

Prell, W.L., 1982. Oxygen and carbon isotope stratigraphy for the Quaternary of Hole 502B: evidence for two modes of isotopic variability. *In* Prell, W.L., Gardner, J.V., et al., *Init. Repts. DSDP,* 68: Washington (U.S. Govt. Printing Office), 455–464.

Raymo, M.E., Oppo, D.W., and Curry, W., 1997. The mid-Pleistocene climate transition: a deep sea carbon isotopic perspective. *Paleoceanography,* 12:546–559.

Schmieder, F., von Dobeneck, T., and Bleil, U., 2000. The mid-Pleistocene climate transition as documented in the deep South Atlantic Ocean: initiation, interim state and terminal event. *Earth Planet. Sci. Lett.,* 179:539–549.

Schönfeld, J., 1996. The "*Stilostomella* Extinction": structure and dynamics of the last turnover in deep-sea benthic foraminiferal assemblages. *In* Mogurlevsky, A., and Whatly, R. (Eds.), *Microfossils and Oceanic Environments:* Aberystwth (Univ. Wales, Aberystwth Press), 27–37.

Schulz, M., and Stattegger, K., 1997. Spectral analysis of unevenly spaced paleoclimatic time series. *Comput. Geosci.,* 23:929–945.

Thompson, P.R., 1981. Planktonic foraminifera in the western North Pacific during the past 150,000 years: comparison of modern and fossil assemblages. *Palaeogeogr., Palaeoclimatol., Palaeoecol.,* 35:241–279.

Wang, L., Sarnthein, M., Erlenkeuser, H., Grimalt, J., Grootes, P., Heilig, S., Ivanova, E., Kienast, M., Pelejero, C., and Pflaumann, U., 1999. East Asian monsoon climate during the late Pleistocene: high-resolution sediment records from the South China Sea. *Mar. Geol.,* 156:245–284.

Wang, L., and Wang, P., 1990. Late Quaternary paleoceanography of the South China Sea: glacial/interglacial contrasts in an enclosed basin. *Paleoceanography,* 5:77–90.

Wang, P., 1999. Response of Western Pacific marginal seas to glacial cycles: paleoceanographic and sedimentological features. *Mar. Geol.,* 156:5–39.

Wang, P., Prell, W.L., Blum, P., et al., 2000. *Proc. ODP, Init. Repts.,* 184 [CD-ROM]. Available from: Ocean Drilling Program, Texas A&M University, College Station TX 77845-9547, USA.

Wang, P., Tian, J., and Cheng, X., 2001. Transition of Quaternary glacial cyclicity in deep-sea records at Nansha, the South China Sea. *Sci. China, Ser. D: Earth Sci.,* 44:926–933.

Wang, R., and Abelman, A., 2002. Radiolarian responses to paleoceanographic events of the southern South China Sea during the Pleistocene. *Mar. Micropaleontol.,* 46:25–44.

Xu, J., Wang, P., Huang, B., Jian, Z., and Li, Q., 2005. Response of planktonic foraminifera to glacial cycles: mid-Pleistocene change in the southern South China Sea. *Mar. Micropaleontol,* 54:89–105.

Zhao, Q., Jian, Z., and Li, B., 1999. Microtektites in the middle Pleistocene deep-sea sediments of the South China Sea. *Sci. China, Ser. D: Earth Sci.*, 42:532–535.

APPENDIX

Quantitative counts of planktonic foraminifers in mid-Pleistocene samples are shown in Table AT1.

AT1. Foraminifer counts, p. 21.

Figure F1. Location of Site 1144 and other sites in the South China Sea.

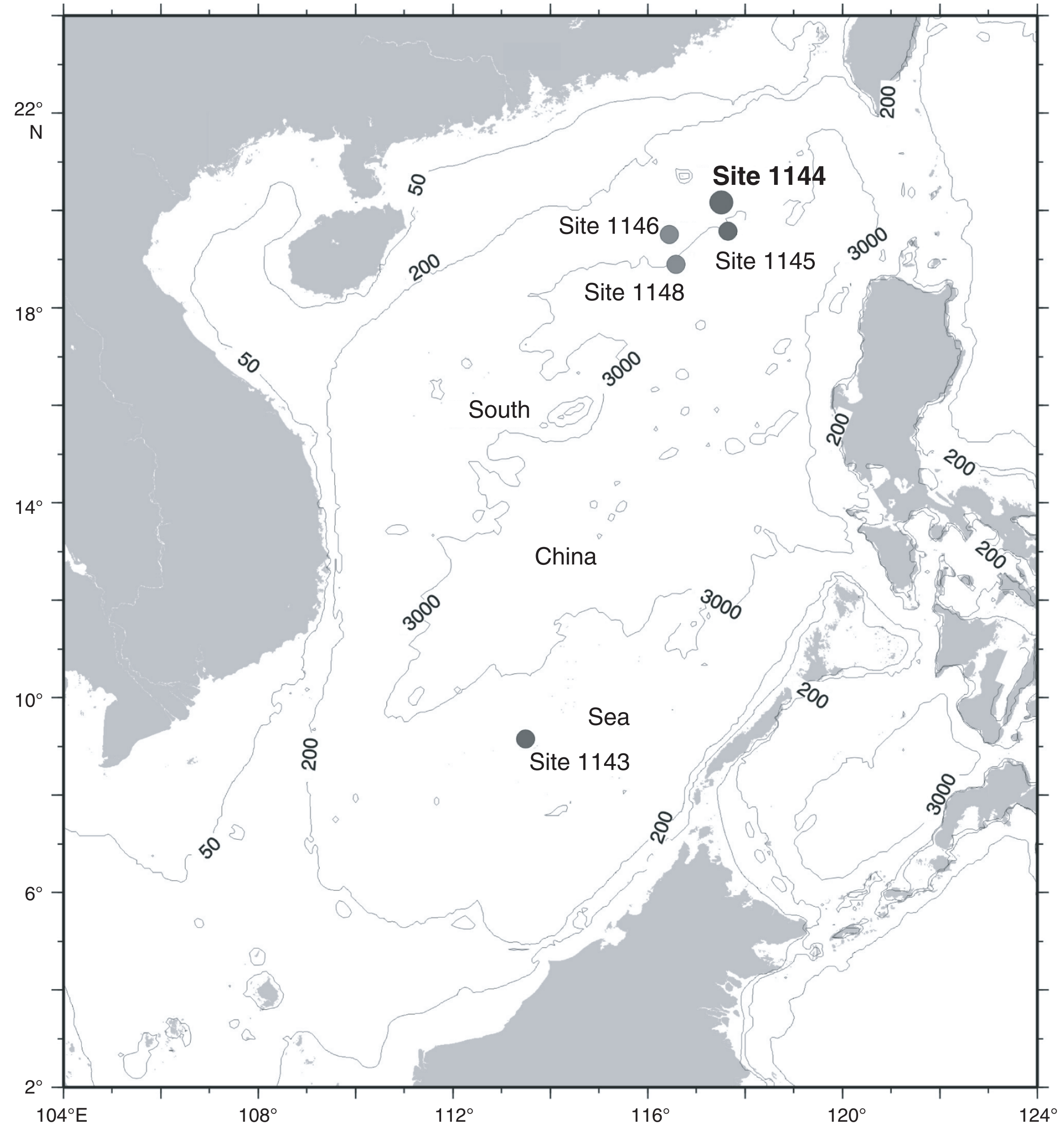

Figure F2. Oxygen isotopic results (Bühring et al., this volume), coarse fraction, planktonic foraminifer abundance, fragment and foraminifer dissolution index, and warm/cold water ratio for the interval between 300 and 518 mcd. Marine isotope Stages (MIS) 14–29 are shaded and labeled. FDX = faunal dissolution index, FO = first occurrence, LO = last occurrence.

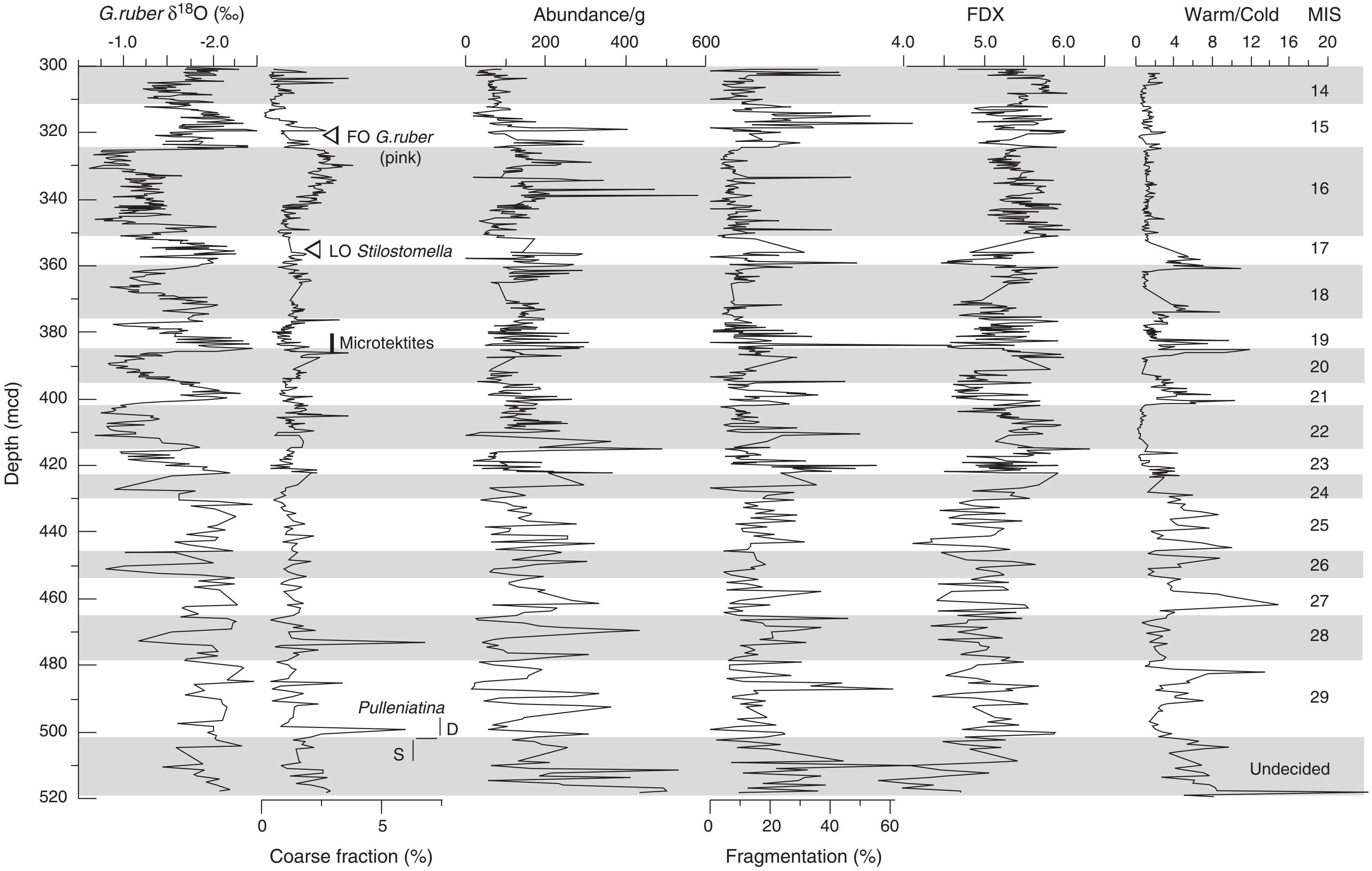

Figure F3. Abundance profiles of the warm-water group and its major constituents. Their abundances decrease uphole with sudden changes across some glacial/interglacial boundaries. MIS = marine isotope stage.

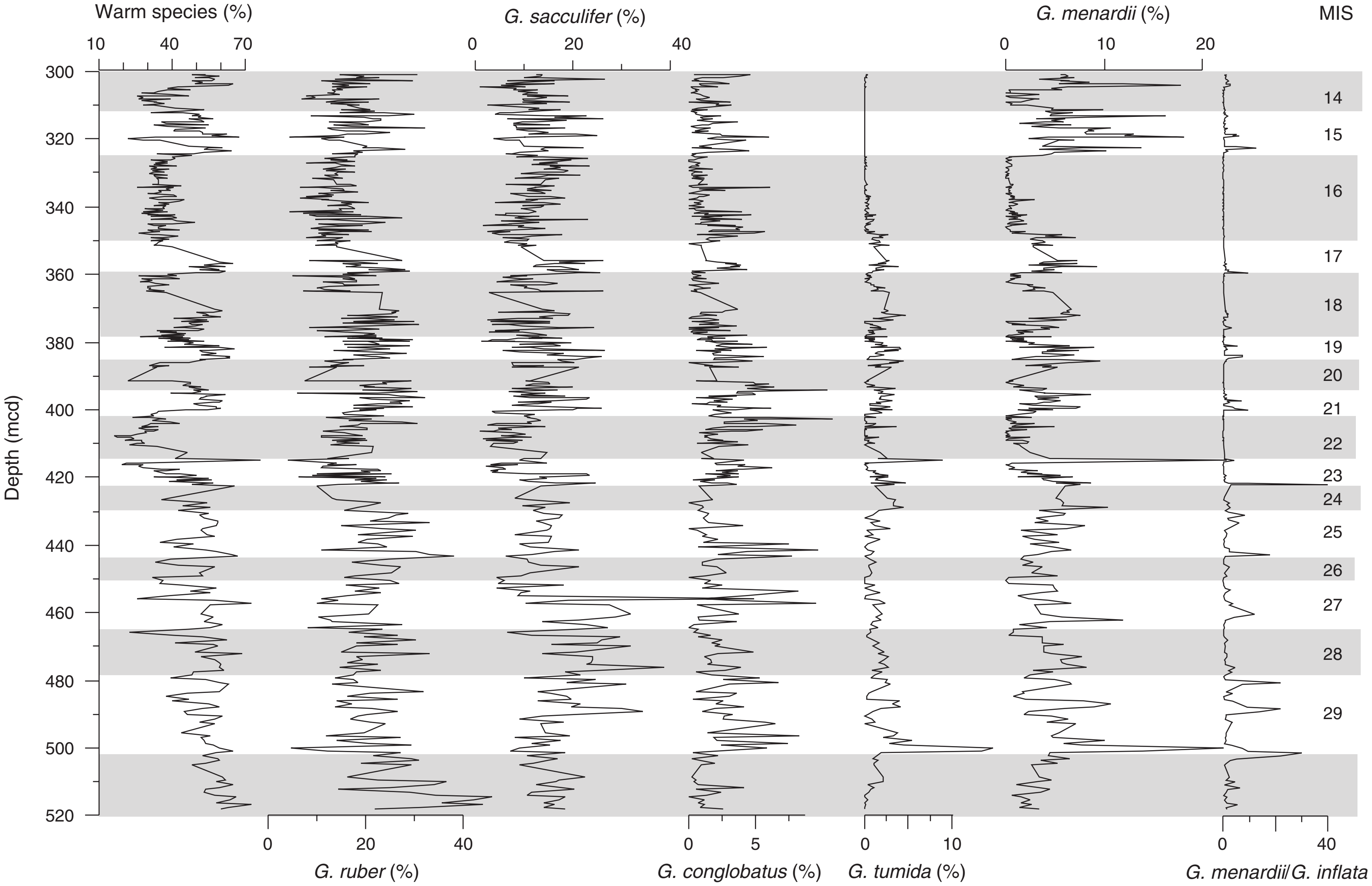

Figure F4. Abundance profiles of the cool- to cold-water group and its main representing species. Their abundances increase uphole, peaking in marine isotope Stage (MIS) 22 at ~70%.

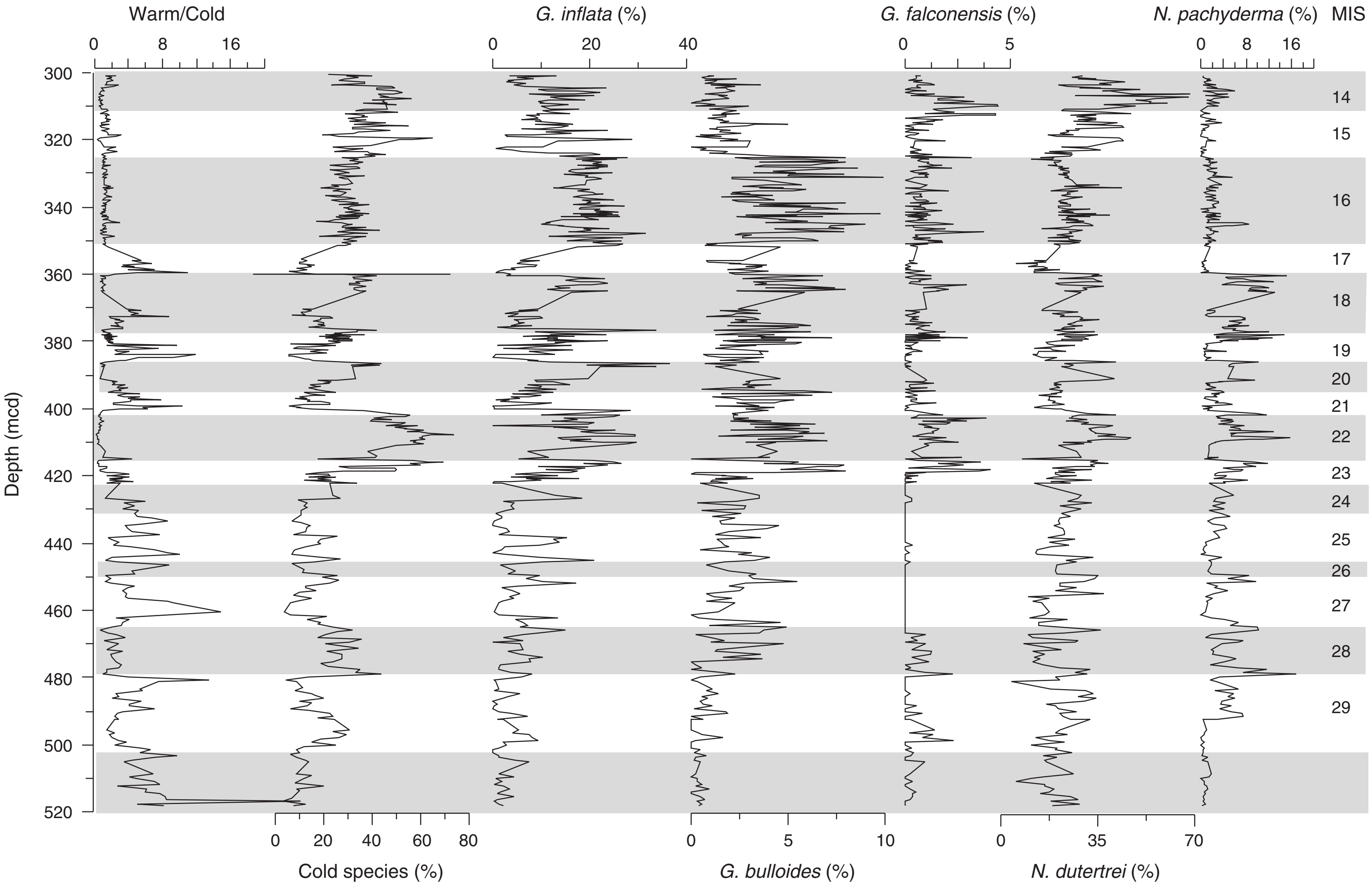

Figure F5. Abundance profiles of *Orbulina, Globigerinella*, and the deep-dwelling group and its representatives. MIS = marine isotope stage.

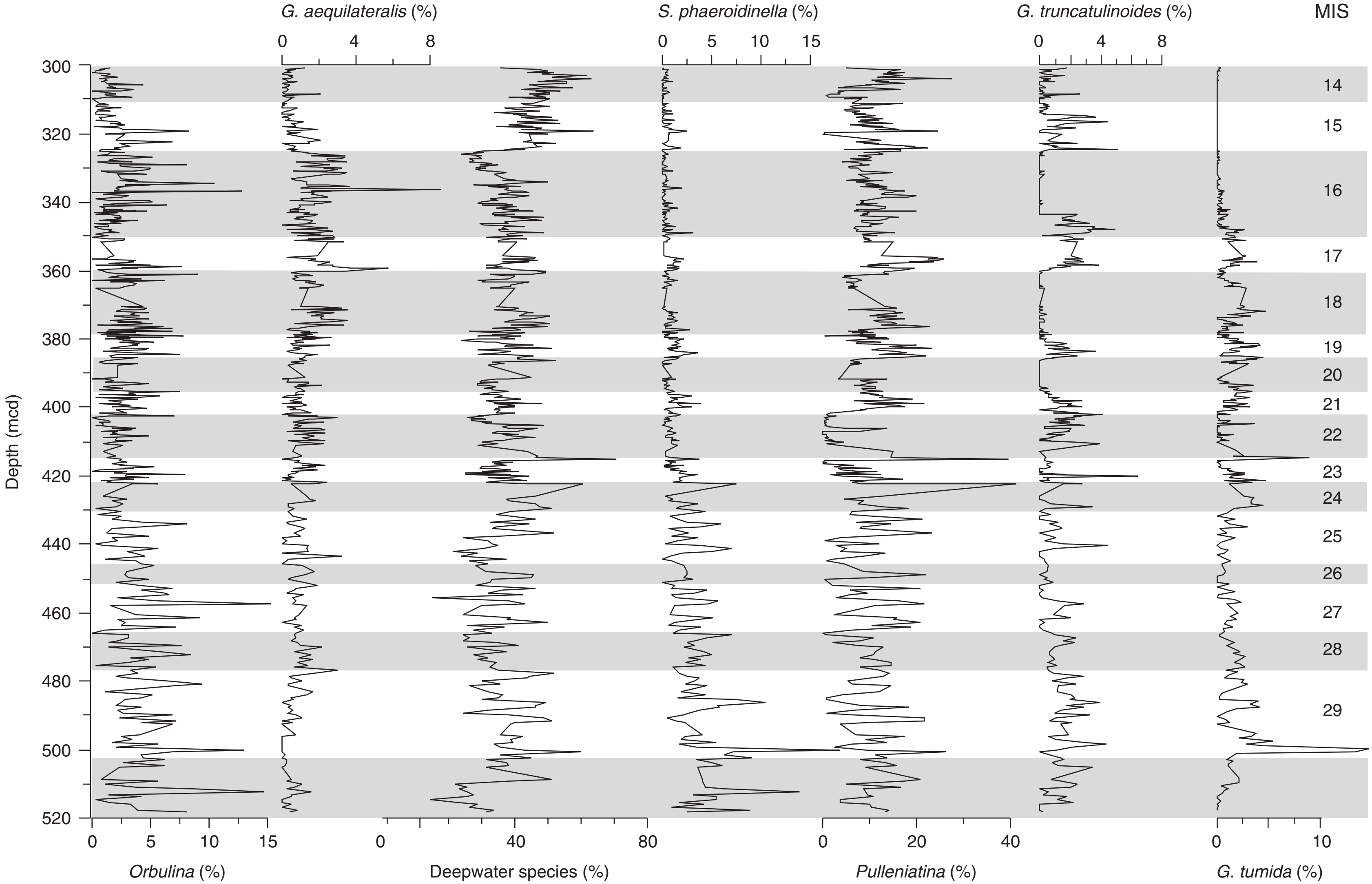

Figure F6. Time plot of $\delta^{18}O$, the estimated winter and summer sea-surface temperatures and their differences, and the abundances of warm-water and deep-dwelling groups. Note distinct transitions of these parameters after ~0.9 Ma. FO = first occurrence, LO = last occurrence, D = dextral, S = sinistral. MIS = marine isotope stage.

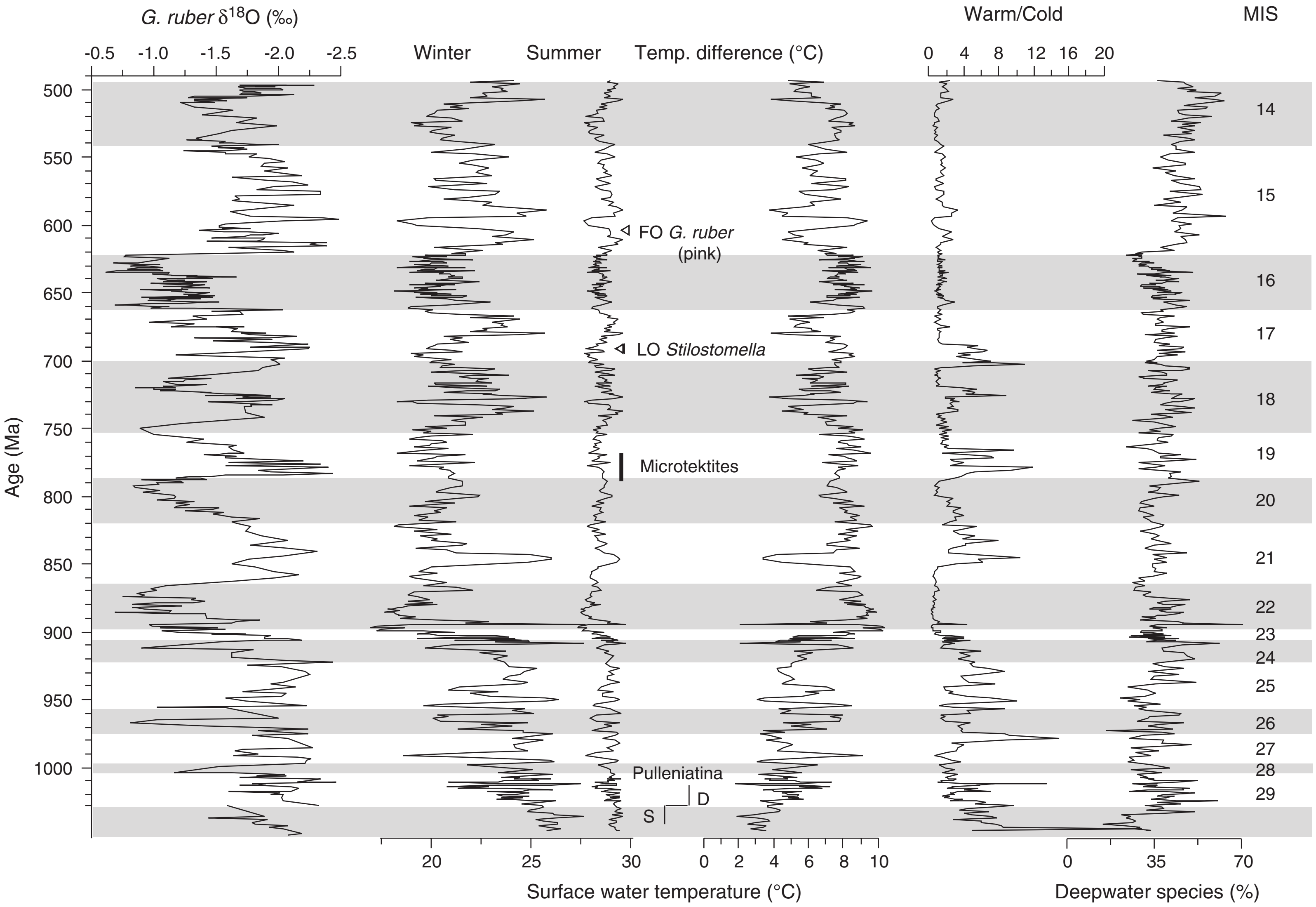

Figure F7. Spectrum analysis of four common planktonic species, showing long (500–100 k.y.) and short (12–6.2 k.y.) cycles. *Globigerinoides ruber* is characterized by a dominant 100-k.y. cycle and many obliquity, precession, and shorter cycles, but lacks the 500-k.y. eccentricity cycle.

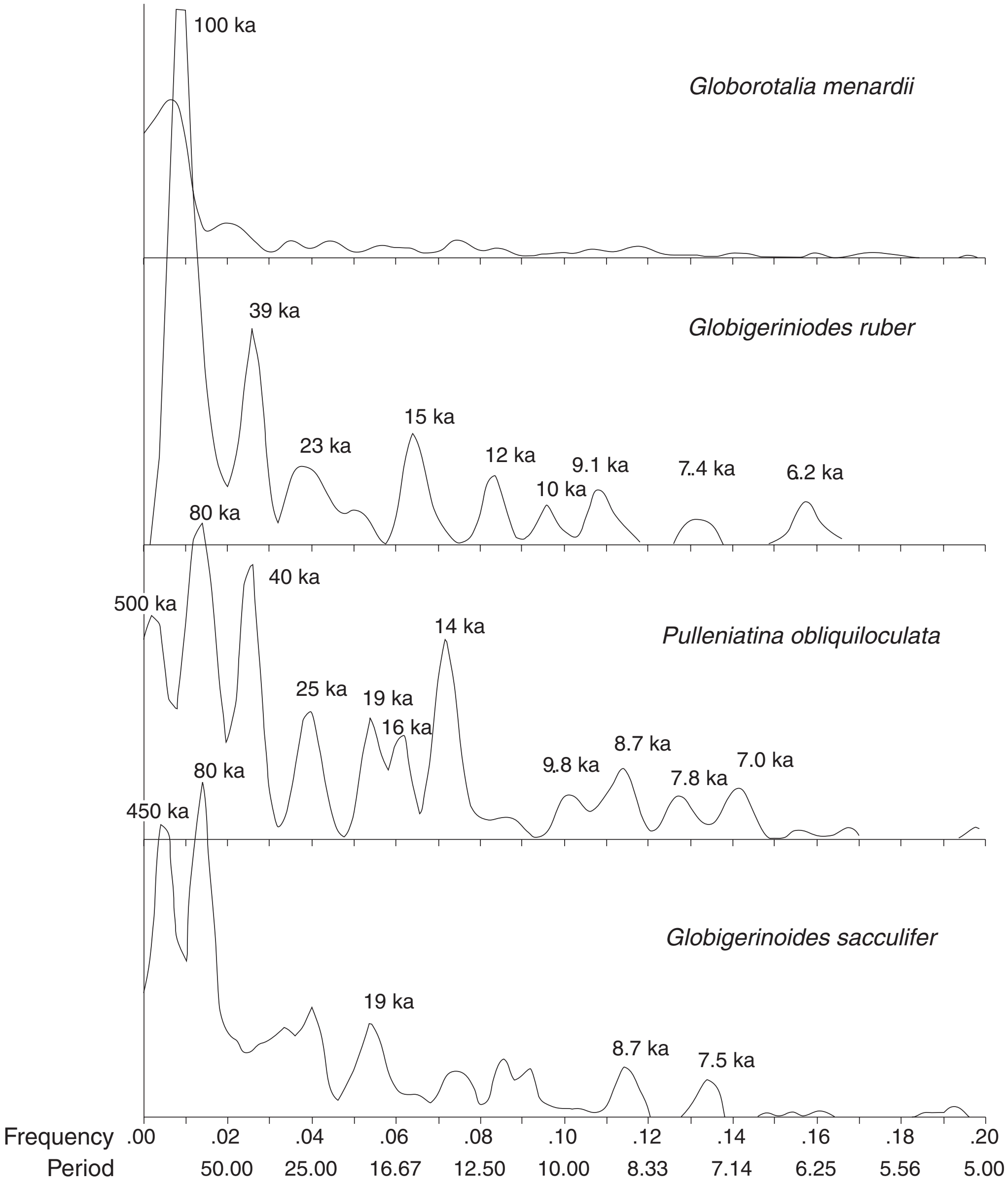

Table T1. Position of marine isotope stages and other events.

MIS	Depth (mcd)	Age (ka)
14	310.8	542
15	325.1	623
16	343.5	656
17	358.7	700
18	374.9	743
19	385	784
20	394.3	815
21	405.4	877
22	418.3	900
23	422.4	907
24	431	920
25	444	954
26	453	975
27	467	995
28	479.1	1007
29	501.3	1022
FO G. ruber pink	313	550
LO Stilostomella	356	690
Microtektites	386	780

Notes: Depth and age calculated at the base of the stage. MIS = marine isotope stage (Buhring et al., this volume). FO = first occurrence, LO = last occurrence.

Table AT1. Quantitative counts of planktonic foraminifers in mid-Pleistocene samples. (This table is available in an **oversized format.**)